

# Seismic inversion for P- and S-wave inverse quality factors using attenuative elastic impedance

Huaizhen Chen\* and Kristopher A. Innanen, Department of Geoscience, University of Calgary, CREWES

## SUMMARY

P- and S-wave inverse quality factors,  $1/Q_P$  and  $1/Q_S$ , quantify seismic wave attenuation, which are related to several key reservoir parameters (porosity, saturation, viscosity, etc.). Estimating  $1/Q_P$  and  $1/Q_S$  from observed seismic data provides additional and useful information for a gas-bearing reservoir prediction. We first derive an approximate reflection coefficient and attenuative elastic impedance involving effects of attenuation, and then we establish an approach to invert for elastic properties (P- and S-wave impedances, and density) and attenuation (P- and S-wave inverse quality factors) from seismic data at different incidence angles and frequencies. The approach includes a model-based and damped least-squares inversion for attenuative elastic impedance, and a Bayesian Markov Chain Monte Carlo inversion for  $1/Q_P$  and  $1/Q_S$ . Synthetic data tests confirm that P- and S-wave impedances and inverse quality factors are reasonably estimated in the case of moderate data error or noise. Applying the established approach to a field data set is suggestive of the robustness of the approach, and that physically meaningful inverse quality factors can be derived from seismic data acquired over a gas-bearing reservoir.

## INTRODUCTION

P- and S-wave velocities and inverse quality factors are related to fluid type and saturation. In gas-bearing reservoirs, higher gas saturation zones often show anomalously high values of attenuation (Chapman et al., 2006). Many rock physics effective models have been developed to show how the fluid affects the attenuation of seismic wave propagation in porous media. Dvorkin and Nur (1993) developed a unified model (BISQ) with the squirt and the Biot mechanisms. Mavko and Jizba (1991) derived formulas for the prediction of high-frequency moduli of a completely saturated rock. Dvorkin et al. (1995) proposed a detailed process to calculate P- and S-wave velocities and inverse quality factors for all frequencies in a fully saturated rock, which is an extension of the Mavko and Jizba (1991) model. Dvorkin and Mavko (2006) developed an approach to calculate P- and S-wave inverse quality factors for the case of partial saturation, based on the standard linear solid model (SLS). In this paper, using the Dvorkin and Mavko (2006) approach, we will estimate P- and S-wave velocities and inverse quality factors at a given reference frequency from well-logging data (porosity, water saturation, minerals and volume, etc.). These quantities are used to generate synthetic data to test the inversion of amplitudes for  $1/Q_P$  and  $1/Q_S$ .

Amplitude variation with frequency (AVF) analysis and inversion can be used to estimate P- and S-wave velocities and inverse quality factors in an attenuative target. Aki and Richards (2002) expressed the frequency-dependent wave velocity in terms of a constant velocity at a reference frequency and inverse quality factor. Innanen (2011) derived absorptive reflection coefficients in terms of perturbations measuring relative changes in density, and P- and S-wave velocities and quality factors across the interface separating an elastic and viscoelastic media. Under the assumption of a constant quality factor, Moradi and Innanen (2015, 2016) described scattering of homogeneous and inhomogeneous seismic waves in low-loss viscoelastic media, and presented linearized expressions of PP- and PS-wave reflection coefficients. However, little effort in pre-stack time-domain frequency-dependent data inversion, for elastic properties (velocity or impedance, density, etc.) and inverse quality factors, has been reported. Under the assumptions of low attenuation and small changes in P- and S-wave inverse quality factors, we make a simplification of the derived PP-wave reflection coefficient and with it present an attenuative elastic impedance (*QEI*). The approach is a two-step inversion, which includes the logarithmic *QEI* inversion from seismic data at different incidence angles and frequencies, and elastic properties and inverse quality factor estimate from the inverted logarithmic *QEI*. Tests on synthetic data indicate that the proposed approach can make a reasonable estimate of P- and S-wave impedances and inverse quality factors in the case of seismic data containing a moderate signal-to-noise ratio (SNR) Gaussian random noise. Applying the approach to a real data set we confirm that it generates meaningful results relevant to gas-bearing reservoir prediction.

## THEORY AND METHOD

### Estimating inverse quality factors from well-logging data

In the Dvorkin and Mavko (2006), the relationship between  $1/Q_P$  and the compressional modulus is given by

$$1/Q_P(\omega) = (M_\infty - M_0)(\omega/\omega_c) / \left\{ \sqrt{M_\infty M_0} \left[ 1 + (\omega/\omega_c)^2 \right] \right\}, \quad (1)$$

where  $M_\infty$  and  $M_0$  are the high- and low-frequency limits of the compressional modulus, and  $\omega_c$  is the critical angular frequency at which the P-wave inverse quality factor reaches its maximum before decreasing.

The  $1/Q_P$  term is re-expressed as

$$1/Q_P(\omega) = 2/Q_P(\omega_c)(\omega/\omega_c) / \left[ 1 + (\omega/\omega_c)^2 \right]. \quad (2)$$

In order to calculate the maximum of  $1/Q_P$ , we calculate  $M_\infty$  and  $M_0$  using well-logging interpretation results

## Estimating inverse quality factors

(minerals and their volumes, porosity, water saturation). After obtaining  $1/Q_P$ , we use an approximate relationship between P- and S-wave inverse quality factors (Mavko et al. 2009) to calculate  $1/Q_S$  directly. A well log model including P- and S-wave impedances ( $I_P$  and  $I_S$ ), density ( $\rho$ ), clay volume ( $V_{SH}$ ), water saturation ( $S_W$ ), and porosity ( $\phi$ ), is displayed in Figure 1.

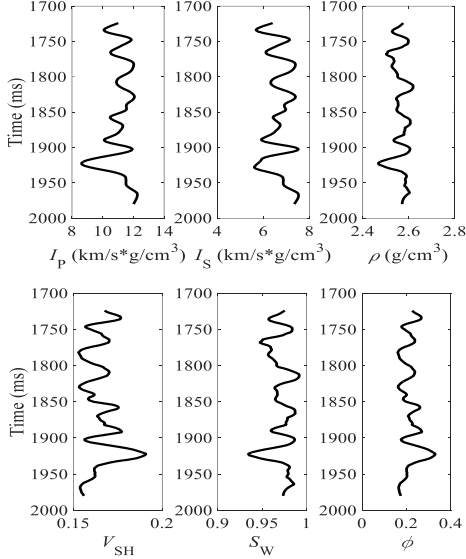


Figure 1. A well log model.

Using Dvorkin and Mavko (2006), we estimate the maximum of  $1/Q_P$  and calculate  $1/Q_S$ ; the results are illustrated in Figure 2.

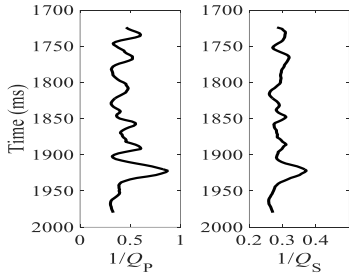


Figure 2. Estimated inverse quality factors.

From Figure 2, we observe high values of  $1/Q_P$  and  $1/Q_S$  which indicate high attenuation, in the vicinity of the gas reservoir (around 1900 ms).

### Complex reflection coefficients and attenuative EI

Aki and Richards (2002) present an expression for the complex wave velocity  $V_{\text{complex}}$  in terms of frequency-

dependent velocity  $V(\omega)$  and  $1/Q(\omega)$ . Given a reference frequency ( $\omega_c$ ), the P-wave velocity is

$$V_p(\omega) = \alpha \left[ 1 + \Gamma(\omega)/Q_p - \psi(\omega)/Q_p i \right], \quad (3)$$

where  $\Gamma(\omega) = 2\psi(\omega)/\pi \log(\omega/\omega_c)$ , and  $\psi(\omega) = \frac{\omega/\omega_c}{1 + (\omega/\omega_c)^2}$ .

The terms  $\alpha$  and  $1/Q_p$  are P-wave velocity and inverse quality factor at the reference frequency  $\omega_c$ . Similarly, the frequency-dependent S-wave velocity is

$$V_s(\omega) = \beta \left[ 1 + \Gamma(\omega)/Q_s - \psi(\omega)/Q_s i \right], \quad (4)$$

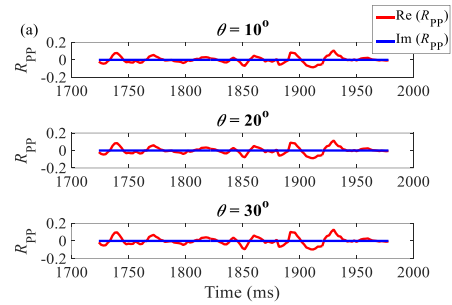
where  $\beta$  and  $1/Q_s$  are S-wave velocity and inverse quality factor at the given reference frequency  $\omega_c$ . Combining equations (3) and (4), we express the frequency-dependent complex stiffness parameters,  $C_{33}(\omega)$  and  $C_{55}(\omega)$  as

$$\begin{aligned} C_{33}(\omega) &= C_{33} \left[ 1 + 2\Gamma(\omega)/Q_p - 2\psi(\omega)/Q_p i \right] \\ C_{55}(\omega) &= C_{55} \left[ 1 + 2\Gamma(\omega)/Q_s - 2\psi(\omega)/Q_s i \right], \end{aligned} \quad (5)$$

where  $C_{33} = \rho \alpha^2$ ,  $C_{55} = \rho \beta^2$ , and  $\rho$  is density. Following Shaw and Sen (2006), we write the complex P-P reflection coefficient using stiffness parameters as

$$\begin{aligned} R_{pp}(\theta, \omega) &= \sec^2 \theta R_p - 8g \sin^2 \theta R_s + (4g \sin^2 \theta - \tan^2 \theta) R_D \\ &+ (2R_p - R_D) \sec^2 \theta \Gamma(\omega)/Q_p + \Gamma(\omega)/2 \sec^2 \theta \Delta(1/Q_p) \\ &- 4(4R_s - 2R_D)g \sin^2 \theta \Gamma(\omega)/Q_s \\ &- 4g \Gamma(\omega) \sin^2 \theta \Delta(1/Q_s) - (2R_p - R_D) \sec^2 \theta \psi(\omega)/Q_p i \\ &- \psi(\omega)/2 \sec^2 \theta \Delta(1/Q_p) i \\ &+ 4g \sin^2 \theta (4R_s - 2R_D) \psi(\omega)/Q_s i \\ &+ 4g \psi(\omega) \sin^2 \theta \Delta(1/Q_s) i \end{aligned} \quad (6)$$

where  $R_p = \Delta I_p / (2I_p)$ ,  $R_s = \Delta I_s / (2I_s)$ , and  $R_D = \Delta \rho / (2\rho)$  are relative changes in P- and S-wave impedances, and density across the interface,  $I_p = \alpha \rho$ ,  $I_s = \beta \rho$ , and  $g = \beta^2 / \alpha^2$ . We next compare the real and imaginary parts of the derived reflection coefficient calculated by using the elastic properties (Figure 1) and the estimated inverse quality factors (Figure 2) at different frequencies and incidence angles. These are shown in Figure 3. We select  $10^4$  Hz as the reference frequency.



## Estimating inverse quality factors

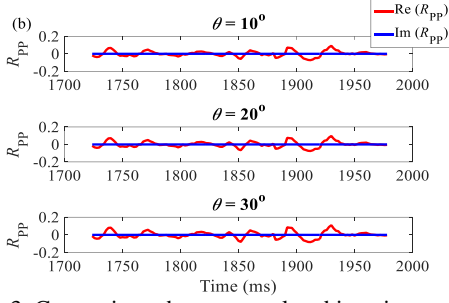


Figure 3. Comparisons between real and imaginary parts. (a) 15 Hz, and (b) 45 Hz.

Neglecting the imaginary part, we derive an attenuative elastic impedance ( $QEI$ ) using the derived reflection coefficient. The logarithmic  $QEI$  ( $LQEI$ ) is given by

$$LQEI(\theta, \omega) = \sec^2 \theta \ln I_p - 8g \sin^2 \theta \ln I_s + \begin{pmatrix} 4g \sin^2 \theta \\ -\tan^2 \theta \end{pmatrix} \ln \rho + \Gamma(\omega) \sec^2 \theta \begin{bmatrix} 2 \ln I_p \\ -\ln \rho \end{bmatrix} \frac{1}{Q_p} - 8g \Gamma(\omega) \sin^2 \theta \begin{bmatrix} 2 \ln I_s \\ -\ln \rho \end{bmatrix} \frac{1}{Q_s} \quad (7)$$

### Inversion for P- and S-wave inverse quality factors

The estimation of P- and S-wave inverse quality factors from observed seismic data is implemented in two steps: the  $LQEI$  is inverted from near, middle, and far offset/angle seismic data stacked over the incidence angle, and then  $1/Q_p$  and  $1/Q_s$  are estimated from the inverted  $LQEI$ . The relationship between the observed seismic data and the  $LQEI$  is

$$\mathbf{B} = \mathbf{A}\mathbf{X}, \quad (8)$$

where  $\mathbf{B}$  is the input data vector,  $\mathbf{X}$  is the  $LQEI$  vector, and  $\mathbf{A}$  is a linear operator incorporating the wavelet. A damped least-squares inversion algorithm is employed to invert for the  $LQEI$

$$\mathbf{X} = \mathbf{X}_{\text{mod}} + (\mathbf{A}^T \mathbf{A} + \xi \mathbf{I})^{-1} \mathbf{A}^T (\mathbf{B} - \mathbf{A}\mathbf{X}_{\text{mod}}), \quad (9)$$

where  $\mathbf{X}_{\text{mod}}$  is the initial model,  $\mathbf{I}$  is the unit diagonal matrix, and  $\xi$  is the damping factor. After the  $LQEI$  estimate, we apply a Bayesian MCMC inversion method to the estimation of P- and S-wave impedances, density and inverse quality factors. In a Bayesian framework, the posterior probability distribution function,  $P(\mathbf{m}|\mathbf{d})$ , of the model vector  $\mathbf{m}$  given the data vector  $\mathbf{d}$  is expressed as

$$P(\mathbf{m}|\mathbf{d}) \propto P(\mathbf{d}|\mathbf{m})P(\mathbf{m}), \quad (10)$$

where  $P(\mathbf{d}|\mathbf{m})$  is the likelihood function, and  $P(\mathbf{m})$  is a prior probability. The nonlinear forward model is given by

$$\mathbf{d} = \mathbf{G}(\mathbf{m}), \quad (11)$$

where  $\mathbf{d}$  is the estimated  $LQEI$  vector,  $\mathbf{G}(\cdot)$  is the forward modeling operator, and  $\mathbf{m}$  is the unknown parameter vector. Given Gaussian noise, we have

$$P(\mathbf{d}|\mathbf{m}) = 1 / (2\pi\sigma_e^2)^N \exp\left\{-\sum [\mathbf{d} - \mathbf{G}(\mathbf{m})]^2 / (2\sigma_e^2)\right\}, \quad (12)$$

where  $(\sigma_e)^2$  is the noise variance. The Cauchy distribution is used as a prior (Alemie and Sacchi, 2011):

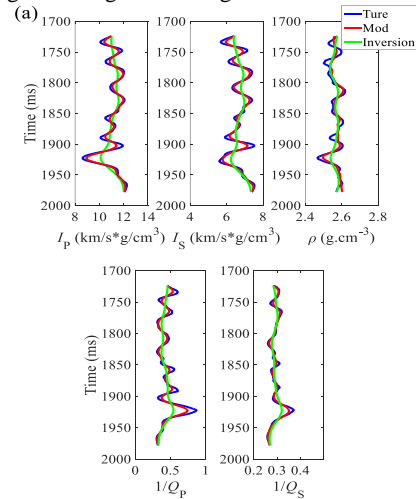
$$P(\mathbf{m}) = 1 / (\pi\sigma_m^2)^N \exp\left\{-\sum \ln [1 + (\mathbf{m} - \Psi_m)^2 / \sigma_m^2]\right\}, \quad (13)$$

where  $\Psi_m$  is the mean value of the unknown parameter vector, and  $\sigma_m^2$  is the variance value of the model parameter vector. A Markov chain Monte Carlo (MCMC) method is employed to generate samples from a probability distribution. We employ the Metropolis-Hastings algorithm to control the transition from the current Markov chain to the next chain, and adopt chains satisfying the acceptance probability. We produce one random variate, and compare it with the acceptance probability. If the random variate is less than the acceptance probability, we accept the candidate chain, otherwise, we reject it and generate a new candidate. The mean values of all accepted candidate chains are used as parameter estimates.

## EXAMPLES

### Synthetic examples

P- and S-wave impedances, density, and inverse quality factors (shown in Figures 1 and 2), and a Ricker source wavelet, are used to generate synthetic seismic gathers. We use the real part of (6) to calculate values of P-P reflection coefficient. After the  $LQEI$  inversion, we estimate P- and S-wave impedances, density, and inverse quality factors with the proposed Bayesian MCMC algorithm as outlined above. Figure 4 shows comparisons between true values (blue) and inversion results (red) of the parameters. P- and S-wave impedances and  $1/Q_p$ ,  $1/Q_s$  are accurately estimated given moderate SNR. The accuracy of the density inversion can likely be improved by involving more large-offset/angle data in the inversion.



## Estimating inverse quality factors

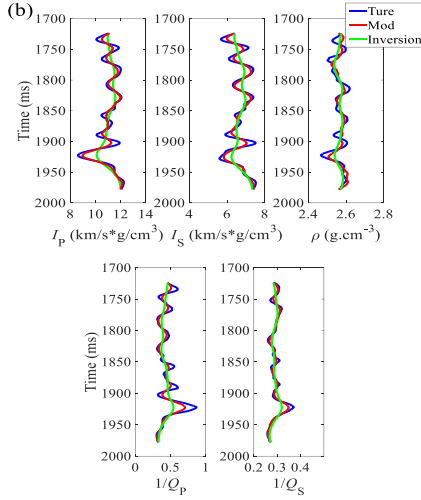


Figure 4. Comparisons between inversion results (red) and true values (blue). Green color represents the initial model. (a) SNR is 5, and (b) SNR is 2.

### Field data example

We analyze a field data set acquired above a gas reservoir in China. We first use seismic data stacked over the incidence angle at different frequencies to invert for the  $LQEI$ , and then we extract P- and S-wave impedances, density, and inverse quality factors using the Bayesian MCMC method. Figure 5 summarizes the inversion results for estimation of P- and S-wave impedances, density, and inverse quality factors. The curve in each figure is the well-logging P-wave velocity.

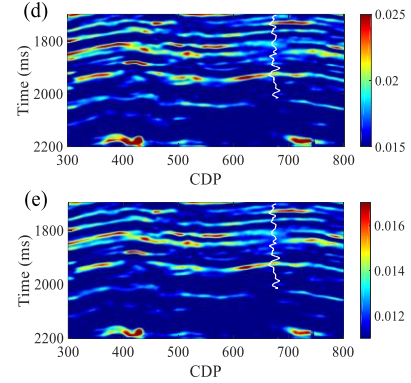
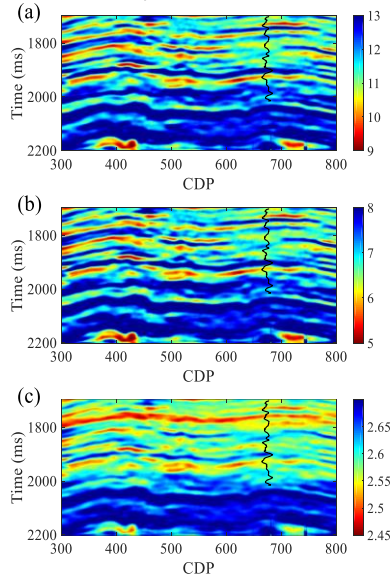


Figure 5. Inversion results of  $I_P$ ,  $I_S$ ,  $\rho$ ,  $1/Q_P$  and  $1/Q_S$ . The curve is P-wave velocity provided by the well log.

(a)  $I_P$ , (b)  $I_S$ , (c)  $\rho$ , (d)  $1/Q_P$  and (e)  $1/Q_S$ .

We observe that at the location of the gas reservoir (around 1900 ms) P- and S-wave impedances and density exhibit low values, and  $1/Q_P$ ,  $1/Q_S$  show high values, which agrees well with the variation of the well-logging P-wave velocity. By incorporating both impedances and the inverse quality factors, we believe the robustness of detection of a gas-bearing reservoir has been increased.

## CONCLUSIONS

We have established an approach to simultaneously invert for elastic (P- and S-wave impedances, and density) and attenuation (P- and S-wave inverse quality factors) properties from observed seismic data, based on the complex reflection coefficient and an attenuative extension of elastic impedance ( $QEI$ ). The approach involves a model-based damped least-squares inversion for  $LQEI$  from seismic data stacked over the incidence angles at different frequencies, and a Bayesian Markov Chain Monte Carlo (MCMC) inversion for  $1/Q_P$  and  $1/Q_S$  from the inverted  $LQEI$ . Synthetic tests verify that unknown parameters can be inverted to produce geologically reasonable values in the case of moderate noise. In application to a field data set, we conclude that by incorporating both impedances and the inverse quality factors in a modified elastic impedance formulation leads to meaningful and efficient gas reservoir detection and characterization.

## ACKNOWLEDGMENTS

The industrial sponsors of CREWES are thanked for their support, as is NSERC (Natural Science and Engineering Research Council of Canada, through the grant CRDPJ 461179-13. We thank the SINOPEC Key Lab of Multi-component Seismic Technology for providing the field data set.